Pure and Applied Mathematics Quarterly
Volume 14, Number 1, 27–55, 2018

Hybrid Fourier-Continuation method and WENO-Z finite difference scheme for multi-dimensional detonation structure simulations

Peng Li, Zhen Gao*, and Wai Sun Don

Abstract: In (Li et al. J. Sci. Comput. 2015, **64**: 670–695), a Hybrid FC-WENO-Z scheme (Hybrid) conjugating the Fourier-Continuation (FC) method with the improved fifth order characteristic-wise weighted essentially non-oscillatory (WENO-Z) finite difference scheme for solving the system of hyperbolic conservation laws was developed. The Hybrid scheme is used to keep the solutions parts displaying high gradients and discontinuities always captured by the WENO-Z scheme in an essentially non-oscillatory manner while the smooth parts are highly resolved by a linear, essentially non-dissipative and non-dispersive FC method. A high order multi-resolution algorithm by Harten is used for measuring the smoothness of the solutions. In this study, the Hybrid scheme is employed in the long time simulations of multi-dimensional detonation structures which contain both discontinuous and complex smooth structures for the first time. The fine scale structures behind the detonation front and the quasi-steady state cellular structures of the peak pressure in the half reaction zone are well captured. A classical stable two-dimensional detonation waves shows that an improved resolution of the more fine scale structures of detonation waves as computed by the Hybrid scheme with less CPU times when compares with the pure WENO-Z scheme. The influence of initial and boundary conditions on the formation and evolution of the detonation structures are also illustrated with examples. Finally, the in-phase rectangular, out-of-phase rectangular and in-phase diagonal cellular structures in the three-dimensional detonation simulations are shown to demonstrate the ability of the Hybrid scheme in capturing the intrinsic evolution of the detonation fronts, which are in good agreement with the published results in the literature.

Keywords: Weighted essentially non-oscillatory, Fourier-Continuation, multi-resolution, Hybrid, detonation wave structures.

Received June 15, 2017.

*Corresponding author.

1. Introduction

Detonation is a type of combustion involving a supersonic exothermic front accelerating through a medium that eventually drives a shock front propagating directly in front of it. It usually occurs in both conventional solid and liquid explosives [13], as well as in the reactive gases. Gaseous detonations are often associated with a mixture of fuel and oxidant in a composition somewhat below conventional flammability ratios. We refer to the website[1] for more descriptions on the detonation theories and applications. However, direct experiments of the detonations, which exists in the most challenging and hostile environment, are difficultly conducted if and when possible. Accurate and efficient numerical simulations of a mathematical model of the detonation waves provide a way to obtain insights in the physical problems and guide researchers to have a deeper understanding of the physics and to design better experiments.

Numerical simulations of the unsteady detonation require solving the system of hyperbolic conservation laws with a reactive source term. The solution of such nonlinear system could develop finite time singularities and create both fine complex smooth and large strong gradient flow structures dynamically in space and time. Direct numerical simulations of fine scale and delicate structures of detonation waves demand the use of highly accurate and efficient numerical schemes, which must be able to resolve a very broad range of length and time scales. For example, second order Godunov scheme [1, 37], extended space-time Conservation Element (CE) and Solution Element (SE) method [44], unsplit scheme [33], non-MUSCL-type TVD scheme [39], classical WENO-JS scheme [12, 41, 42, 43] and optimal WENO-Z scheme [18, 19] have been implemented to simulate detonation waves under different research backgrounds. The grid convergence study for the case of overdrive factor $f = 1.6$ in [18] showed that the WENO schemes converge faster than other existing numerical methods such as PPM with front tracking and mesh refinement [4], unsplit scheme [32], Roe's solver with minmod limiter [34] and Roe's solver with superbee limiter [34].

However, the WENO scheme is highly complex to implement and computationally expensive as it requires, at each grid point, the setup of the Roe-averaged eigensystem, the flux splitting, the forward and backward projections between characteristic and physical spaces, the computation of the smoothness indicators and nonlinear weights. The overhead could make the WENO scheme at least five times more expensive than other nonlinear shock

[1] https://en.wikipedia.org/wiki/Detonation

capturing schemes. Moreover, the WENO scheme is, in general, too dissipative for certain class of problems (for example, compressible turbulence) than the linear schemes (for example, compact scheme) at a given order and resolution. Furthermore, the results in [23] have demonstrated clearly that the WENO-Z scheme is not only less dissipative and dispersive but also less sensitive to the random phases than the WENO-JS scheme.

The Fourier-Continuation (FC) method [5, 31] is a high order complex technique for reconstruction of a non-periodical function using the Fourier collocation method on an extended periodical function over an extended domain on an uniformly spaced grid. It has been shown, for a sufficiently smooth non-periodical function, the reconstructed trigonometric function, when used as Fourier collocation method [20] for solving a wave equation with the smooth solution, is of high order and essentially non-dissipative and non-dispersive [5, 31], which is very important in a long time simulation such as the quasi-steady state solution of the detonation waves. However, in the present of high gradients and discontinuities, the numerical oscillations known as the Gibbs phenomena will appear in the solution and might cause instability and loss of accuracy [10].

To alleviate some of these difficulties, a natural way is to avoid using the WENO scheme and to use high order linear scheme in the smooth regions of the solution wherever and whenever possible. In a multi-domain framework [35, 36], the non-dissipative and non-dispersive FC method worked well together with the WENO-Z scheme for solving the system of hyperbolic conservation laws. In [27], we designed a Hybrid FC-WENO-Z scheme for the numerical simulations of the system of hyperbolic conservation laws in a single-domain framework. Many critical and unique numerical issues in an accurate and efficient implementation are discussed there. The accuracy and efficiency of the Hybrid FC-WENO-Z scheme in solving the one- and two-dimensional system of hyperbolic conservation laws was demonstrated with several classical examples of shocked flow, such as the one-dimensional Riemann initial value problems (123, Sod and Lax), the Mach 3 shock-entropy wave interaction problem with a small entropy sinusoidal perturbation, the Mach 3 shock-density wave interaction problem, and the two-dimensional Mach 10 double Mach reflection problem. For a sufficiently large problem size, a factor of almost two has been observed in the speedup of the Hybrid FC-WENO-Z scheme over the WENO-Z scheme.

In this followup work, the main aim is to examine the applicability and performance of the Hybrid FC-WENO-Z scheme, despite the complexity of the algorithm, for the multi-dimensional detonation wave simulations which contain both discontinuities and fine scale complex structures for the first

time. Several classical stable and unstable two-dimensional detonation waves are simulated. The structures behind the detonation front and the quasi-steady state cellular structures of peak pressure in the half reaction zone are used to verify the accuracy and robustness of the proposed scheme. The numerical examples show that more fine scale structures of detonation waves are well resolved by the Hybrid FC-WENO-Z scheme with less CPU times than the pure WENO-Z scheme for a given grid resolution. We study the factors like the initial and boundary conditions, which are related to the propagation and evolution of the detonation waves. The results show that they play a minor role in the width-to-length ratio of the cellular structures of quasi-steady state solution of the detonation waves. Furthermore, we investigate the performance of Hybrid FC-WENO-Z scheme for the three-dimensional simulations of detonation waves and illustrate the in-phase rectangular, out-of-phase rectangular and in-phase diagonal cellular structures that appear in the three-dimensional detonation waves in a square shock tube. For simplicity, we shall refer to the Hybrid FC-WENO-Z scheme simply as the Hybrid scheme in the rest of the paper.

The paper is organized as follows. In Section 2, a brief introduction to the governing equations and its initial and boundary conditions is presented. In Section 3, a brief introduction to the Hybrid scheme for solving the detonation system is given. In Section 4, several two-dimensional classical stable and unstable detonation waves and three-dimensional stable detonation waves are simulated and their results are discussed. Conclusion and future works are given in Section 5.

2. Governing equations

The three-dimensional unsteady reactive Euler equations for a perfect ideal gas coupled with one-step irreversible chemical reaction is given by

$$\frac{\partial \mathbf{Q}}{\partial t} + \boldsymbol{\nabla} \cdot \overrightarrow{\mathbf{F}} = \mathbf{S}, \tag{1}$$

where $\overrightarrow{\mathbf{F}} = (\mathbf{F}, \mathbf{G}, \mathbf{H})$ is the flux vector.

$$\mathbf{Q} = \begin{bmatrix} \rho \\ \rho u \\ \rho v \\ \rho w \\ E \\ \rho f_1 \end{bmatrix}, \mathbf{F} = \begin{bmatrix} \rho u \\ \rho u^2 + P \\ \rho uv \\ \rho uw \\ (E+P)u \\ \rho f_1 u \end{bmatrix}, \mathbf{G} = \begin{bmatrix} \rho v \\ \rho uv \\ \rho v^2 + P \\ \rho vw \\ (E+P)v \\ \rho f_1 v \end{bmatrix}, \tag{2}$$

$$\mathbf{H} = \begin{bmatrix} \rho w \\ \rho u w \\ \rho v w \\ \rho w^2 + P \\ (E+P)w \\ \rho f_1 w \end{bmatrix}, \mathbf{S} = \begin{bmatrix} 0 \\ 0 \\ 0 \\ 0 \\ 0 \\ \omega(T, f_1) \end{bmatrix},$$

where ρ is density, P is pressure, u, v and w are the x-, y- and z-components of velocity vector respectively. $0 \leq f_1 \leq 1$ is the reactant mass fraction. The total specific energy E is given by,

$$E = \frac{P}{\gamma - 1} + \frac{1}{2}\rho(u^2 + v^2 + w^2) + \rho f_1 q_0, \tag{3}$$

where γ is the ratio of specific-heat, and q_0 is the heat-release parameter. The source term $\omega(T, f_1)$ due to the Arrhenius rate law is

$$\omega(T, f_1) = -K\rho f_1 e^{-E_a/T}, \tag{4}$$

where $T = P/(\rho R)$ is the temperature, R is the specific gas constant (with a suitable normalization, $R = 1$ in this study), E_a is the activation-energy parameter, and K is a pre-exponential factor that sets the spatial and temporal scales.

Remark 1. *There are many detonation models such as the one-step simple model based on the Arrhenius rate law [14, 15, 16, 25], the multi-step chain-branching model [28, 29, 38], the detailed chemical reaction model [22]. Generally speaking, the multi-step chain-branching or the detailed reaction model for detailed investigating the mechanism of detonation are necessary. However, Gamezo et al. [14] claimed that almost all of the complex phenomena of detonation can be generated by the one-step Arrhenius kinetics. Therefore, in this study, we use the one-step model for our simulations.*

In this work, we simulate three classical multi-dimensional detonation waves, which are the stable, weakly unstable and highly unstable detonations. The corresponding parameters are listed in Table I, where f is the overdrive factor. The parameters γ, q_0, E_a and f determine the primary state of the detonation waves. We refer to [26] for detailed discussion of the relationship between the detonation structures and these parameters.

In the two- and three-dimensional problems, the y- and z-components of initial velocity are perturbed by a transversely sinusoidal planar ZND wave,

Table I: Cases of simulation and corresponding parameters

Cases studied	Stability in 1D	γ	q_0	E_a	f
Case A	Stable	1.2	2	20	1.1
Case B	Unstable, with one unstable mode	1.2	50	50	1.6
Case C	Unstable, with five unstable mode	1.2	50	50	1.2

i.e.,

$$v(x,y,z,0) = \begin{cases} 0 & x < x_d - W_w \\ A\sin\left(\frac{2y\pi k}{L} + \theta_1\right) & x_d - W_w \le x \le x_d \\ 0 & x > x_d \end{cases},$$

$$w(x,y,z,0) = \begin{cases} 0 & x < x_d - W_w \\ A\sin\left(\frac{2z\pi k}{L} + \theta_2\right) & x_d - W_w \le x \le x_d \\ 0 & x > x_d \end{cases},$$

where A, k, L and θ_i $(i = 1, 2)$ are the amplitude, wave number, wavelength and phases in the y- and z-directions respectively. W_w is the width of perturbation zone. x_d is the initial location of the detonation wave front in the x-direction. L is equal to the length of the physical domain in the y- or z-directions. In this study, $W_w = 1$ is used, the right boundary condition is set to be the initial free stream inflow condition. The perfectly match layer (PML) absorbing boundary condition is created to minimize the reflection wave generated from the left boundary condition. The reflective boundary conditions are imposed in the y- and z-directions. We refer to [19] for details on the initial conditions and the PML absorbing boundary condition.

3. Hybrid FC-WENO scheme

In this section, we briefly introduce the three main components of the Hybrid scheme: WENO-Z scheme, Fourier-Continuation method and multi-resolution analysis in solving the system of hyperbolic conservation laws with source terms (1). We refer to [27] and the references therein for detailed descriptions of the Hybrid scheme. We assume the computational domain as $\Omega_0 = [a, b]$ of length $L = b - a$. The domain is discretized by $N + 1$ equidistant grids with grid spacing $\Delta x = L/N$. The cell centers and boundaries are given by $x_i = a + i\Delta x$ and $x_{i+\frac{1}{2}} = x_i + \frac{\Delta x}{2}$, $i = 0, \ldots, N$ respectively. Three additional ghost points are setup at both ends of the domain.

3.1. The WENO-Z scheme

The semi-discretized form of the convection terms of (1) is transformed into the system of ODEs and solved by the method of lines

$$\frac{dQ_i(t)}{dt} = -\left.\frac{\partial f}{\partial x}\right|_{x=x_i}, \quad i = 0, \ldots, N, \tag{5}$$

where $Q_i(t)$ is a numerical approximation to the cell-averaged value $Q(x_i, t)$. To form the flux difference and to obtain a high-order numerical flux consistent with the hyperbolic conservation laws, a conservative finite difference formulation is required at the cell boundaries. By defining a numerical flux function $h(x)$ implicitly, one has

$$f(x) = \frac{1}{\Delta x}\int_{x-\frac{\Delta x}{2}}^{x+\frac{\Delta x}{2}} h(\xi)d\xi, \tag{6}$$

such that the spatial derivative in (5) is approximated by a conservative finite difference formula at the cell center x_i,

$$\frac{dQ_i(t)}{dt} = -\frac{1}{\Delta x}\left(h_{i+\frac{1}{2}} - h_{i-\frac{1}{2}}\right), \tag{7}$$

where $h_{i\pm\frac{1}{2}} = h(x_{i\pm\frac{1}{2}})$.

We takes the fifth order WENO-Z scheme for example. The 5-points global stencil S^5 is subdivided into three 3-points substencils $\{S_0, S_1, S_2\}$ (see Fig. 1). The fifth degree polynomial approximation $\hat{f}_{i\pm\frac{1}{2}} = h_{i\pm\frac{1}{2}} + O(\Delta x^5)$ is built through the convex combination of three second degree interpolation

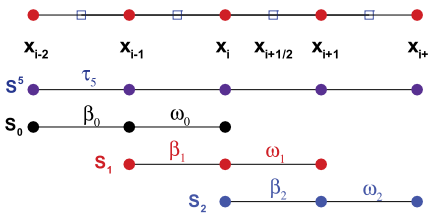

Figure 1: The computational uniformly spaced grid x_i and the 5-points stencil S^5, composed of three 3-points substencils $\{S_0, S_1, S_2\}$, used for the fifth-order WENO reconstruction step.

polynomials $\hat{f}^k(x)$ in substencils $S_k, k = 0, 1, 2$ at the cell boundaries $x_{i+\frac{1}{2}}$,

$$\hat{f}_{i+\frac{1}{2}} = \sum_{k=0}^{2} \omega_k \left(\sum_{j=0}^{2} c_{kj} f_{i-k+j} \right), \tag{8}$$

where ω_k and c_{kj} are the normalized nonlinear weights and the Lagrangian interpolation coefficients [24] respectively. Similar formulation can be derived for $\hat{f}_{i-\frac{1}{2}}$. The nonlinear weights ω_k in the WENO-Z scheme [2, 6, 11] are defined as

$$\alpha_k = d_k \left(1 + \left(\frac{\tau_5}{\beta_k + \epsilon} \right)^p \right), \quad \omega_k = \frac{\alpha_k}{\sum_{l=0}^{2} \alpha_l}, \quad k = 0, 1, 2, \tag{9}$$

where $\tau_5 = |\beta_2 - \beta_0|$, β_k is the local smoothness indicators which measure the regularity of the second degree interpolation polynomial in substencils $S_k, k = 0, 1, 2$. The coefficients $\{d_0 = \frac{3}{10},\ d_1 = \frac{3}{5},\ d_2 = \frac{1}{10}\}$ are the ideal weights, such that when the solution is sufficiently smooth, one has $\{\omega_k \approx d_k, k = 0, 1, 2\}$. The power parameter $p = 2$ and the sensitivity parameter $\epsilon = 10^{-16}$ are used in this study.

Remark 2. *The polynomial reconstruction procedure is applied to the characteristic projection of the positive and negative fluxes after applying the global Lax-Fredrichs flux splitting of the Euler flux above.*

3.2. The Fourier-Continuation method

In the Fourier-Continuation (FC) method, as shown in Fig. 2, we shall take a smooth non-periodical function $f(x)$ defined over a domain $\Omega_0 = [a, b]$ for example. The definition of $f(x)$ is then extended to a new periodical function $h(z)$ with period $L + d$ over an extended periodical domain $\Omega_2 = \Omega_0 \bigcup \Omega_1 = [a, b + d]$, that is,

$$h(z) = \begin{cases} f(z) & z \in \Omega_0 = [a, b] \\ f_{\texttt{match}}(z) & z \in \Omega_1 = [b, b + d] \end{cases}, \tag{10}$$

where d is a parameter that determines the size of the domain Ω_1. $f_{\texttt{match}}(z)$ is a matching *periodical* function defined over a matching *periodical* domain

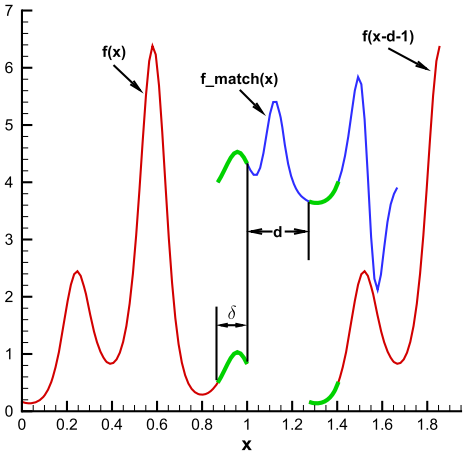

Figure 2: Setup of the FC method of a non-periodical function $f(x)$ (red line) in the domain $[0, 1]$. Raised for visibility, the matching periodical function $f_{\texttt{match}}(x)$ (blue and green lines) is displayed in the upper-right portion of the figure.

$\Omega_3 = [b - \delta, b + 2d + \delta]$ with period $2(d + \delta)$ and satisfies

(11)

$$f_{\texttt{match}}(z) = \begin{cases} f(x) & x \in [b-\delta, b] \quad \text{and} \quad z \in \Omega_{\texttt{left}} = [b-\delta, b] \\ f(x) & x \in [a, a+\delta] \quad \text{and} \quad z \in \Omega_{\texttt{right}} = [b+d, b+d+\delta] \end{cases},$$

where δ is a parameter that determines the length of an overlapped subdomain between $f(x)$ and $f_{\texttt{match}}(z)$.

Since we are using the Fourier collocation method [20], the grid spacing Δx must remain unchanged on Ω_2. Hence, the parameters d and δ must be in a form of $d = \gamma \Delta x$ and $\delta = \beta \Delta x$, for some non-zero positive integers γ and β. Therefore, the Fourier collocation points z_j on Ω_1 must then be defined accordingly as $z_j = b + j\Delta x, j = 0, \ldots, \gamma$.

In the left overlapped subdomain $\Omega_{\texttt{left}} = [b - \delta, b]$, instead of forcing the matching function $f_{\texttt{match}}(z) = f(x)$ strictly, $f(x)$ is approximated by the orthogonal Gram polynomial [8] to some desirable accuracy, provided that the degree of the Gram polynomial M is not too large (says, $M \leq 10$),

(12)

$$f_{\texttt{match}}(z) = \sum_{n=0}^{M} f_n^{\texttt{left}} P_n^{\texttt{left}}(\xi), \quad f_n^{\texttt{left}} = \sum_{i=0}^{\beta} f_{\texttt{match}}(z_i) P_n^{\texttt{left}}(\xi_i), \quad M \leq \beta,$$

$$\xi = -1 + \frac{2}{\delta}(z - (b - \delta)), \quad z \in \Omega_{\texttt{left}}, \tag{13}$$

where $P_n^{\texttt{left}}(\xi)$ are the Gram polynomials of degree n and $f_n^{\texttt{left}}$ are the $n_$th Gram coefficients. Similarly, in the right overlapped subdomain $\Omega_{\texttt{right}} = [b + d, b + d + \delta]$, one can obtain the corresponding $P_n^{\texttt{right}}(\xi)$ and $f_n^{\texttt{right}}$.

To obtain the Fourier continuation of the *periodical* matching function $f_{\texttt{match}}(z)$ in domain $\Omega_3 = [b - \delta, b + 2d + \delta]$ with period $2(d + \delta)$ that satisfies the matching conditions (11) in the overlapped subdomain $\Omega_{\texttt{left}}$ and $\Omega_{\texttt{right}}$, we discretize the domain $\Omega_{\texttt{left}} = [b - \delta, b]$ with $R + 1$ equidistant grid points, namely, $z_l = b - \delta + l\Delta z, l = 0, \ldots, R$. We then define an even function $f_n^{\texttt{even}}(z)$ and an odd function $f_n^{\texttt{odd}}(z)$ such that

$$f_n^{\texttt{even}}(z_\ell) = \sum_{k \in t_{\texttt{even}}(K)} \hat{a}_k^n e^{i\frac{\pi k}{\delta + d} z_\ell} \approx P_n^{\texttt{left}}(\xi_\ell), \ \ell = 0, \cdots, R, \tag{14}$$

$$f_n^{\texttt{odd}}(z_\ell) = \sum_{k \in t_{\texttt{odd}}(K)} \hat{b}_k^n e^{i\frac{\pi k}{\delta + d} z_\ell} \approx P_n^{\texttt{left}}(\xi_\ell), \ \ell = 0, \cdots, R, \tag{15}$$

where $z_\ell \in \Omega_{\texttt{left}}$, $\xi_\ell = -1 + \frac{2}{\delta}(z_\ell - (b - \delta))$, $t_{\texttt{even}}(K) = \{j \in t(K) | \mod (j, 2) = 0\}$ and $t_{\texttt{odd}}(K) = \{j \in t(K) | \mod (j, 2) = 1\}$ where $t(K) = \{j \in \mathbb{N}, \mod (K, 2) = 0 | -K/2 + 1 \le j \le K/2\}$ or $t(K) = \{j \in \mathbb{N}, \mod (K, 2) = 1 | -(K - 1)/2 \le j \le (K - 1)/2\}$, and K is a user tunable parameter for accuracy in approximating the Gram polynomials with the $[K/2]$ Fourier modes. One can easily verify that $f_n^{\texttt{even}}(z) = f_n^{\texttt{even}}(z + d + \delta)$ and $f_n^{\texttt{odd}}(z) = -f_n^{\texttt{odd}}(z + d + \delta)$ for all n and $z \in \Omega_{\texttt{left}}$. The system (14) and (15) above must be solved in a least square sense since the system is an over-determined system of linear equations. We compute the singular value decomposition (SVD) of a complex matrix with element $A_{k\ell} = e^{i\frac{\pi k}{\delta + d} z_\ell}$. To improve the conditioning of the over-determined system of linear equations, we reset those singular values to zero if they are smaller than a certain user defined threshold $\varepsilon_{\texttt{SVD}}$, for example, $\varepsilon_{\texttt{SVD}} = 10^{-11}$.

Once the functions $f_n^{\texttt{even}}(z)$ and $f_n^{\texttt{odd}}(z)$ have been determined, the matching function $f_{\texttt{match}}$ can be obtained by means of the linear combination as,

$$f_{\texttt{match}}(z) = \sum_{n=0}^{M} \left[\frac{f_n^{\texttt{left}} + f_n^{\texttt{right}}}{2} f_n^{\texttt{even}}(z) + \frac{f_n^{\texttt{left}} - f_n^{\texttt{right}}}{2} f_n^{\texttt{odd}}(z) \right]. \tag{16}$$

We refer to [5, 31] and references therein for a more detailed discussion of the theoretical development, practical implementation, and application of the FC method.

In this work, the parameters $\beta = 10$, $\gamma = 19$, $M = 6$, $R = 100$, $K = 30$ are used. A fast transform algorithm, which uses a version of fast Fourier transform (FFT) algorithm [30], is applied to perform the Fourier differentiation of $h(z)$ to obtain $h'(x)$ which approximates $f'(x)$ [27].

3.3. Multi-resolution analysis

To quantify the smoothness of a solution at each grid point x_i, the coefficients of the Multi-Resolution (MR) analysis [21] can be used.

Given an initial number of the grid points N_0 and grid spacing Δx_0, we shall consider a set of nested dyadic grids up to level $L < \log_2 N_0$,

$$G^k = \{x_i^k, \quad i = 0, \ldots, N_k\}, \quad 0 \le k \le L, \tag{17}$$

where $x_i^k = i\Delta x_k$ with $\Delta x_k = 2^k \Delta x_0$, $N_k = 2^{-k} N_0$ and the cell averages of function u at x_i^k:

$$\bar{u}_i^k = \frac{1}{\Delta x_k} \int_{x_{i-1}^k}^{x_i^k} u(x)dx, \tag{18}$$

Let $\tilde{u}_{2i-1}^k$ be the approximation to $\bar{u}_{2i-1}^k$ by a unique polynomial of degree $n_{MR} = 2s$ that interpolates $\bar{u}_{i+l}^k, |l| \le s$ at x_{i+l}^k, where $q = 2s + 1$ is the order of approximation.

The multi-resolution coefficients, taking $k = 1$ for a single-level MR, $d_i = \bar{u}_{2i-1}^0 - \tilde{u}_{2i-1}^0$ at x_i, has the property that if $u(x)$ is a C^{p-1} function, then

$$d_i \approx \begin{cases} [u_i^{(p)}]\Delta x_1^p & p \le q \\ u_i^{(q)} \Delta x_1^q & p > q \end{cases}, \tag{19}$$

where $[\cdot]$ and $(\cdot)$ denote the jump and the derivatives of the function, respectively. The MR coefficient d_i measures how close the data at the finer grid $\{x_i^0\}$ can be interpolated by the data at the coarser grid $\{x_i^1\}$. It follows that

$$|d_{2i}| \approx 2^{-\bar{p}} |d_i|, \quad \bar{p} = \min\{p, q\}, \tag{20}$$

which implies that away from discontinuities, the MR coefficients $\{d_i\}$ diminish in size with a refinement of the grid at smooth parts of the solution; close to discontinuities, they remain essentially the same size, independent of the order $q = 2s+1$. Examples of the performance of the MR analysis in detecting discontinuities in the solution of nonlinear system of hyperbolic PDEs can be found in [7].

3.4. The Hybrid scheme algorithm

Algorithmically, the Hybrid scheme is implemented with the following essential steps:

1. Perform a n_{MR} (Typically $n_{MR} = 2r$) order multi-resolution (MR) analysis [21, 7] on one or more suitable variable(s) (Density is used in this study) once at the beginning of a time stepping scheme.
2. Set a MR flag `Flag`, based on the MR coefficients d_i, at a grid point x_i as

$$\texttt{Flag}_i = \begin{cases} 1, & |d_i| > \epsilon_{MR} \quad \text{(non-smooth stencil)}, \\ 0, & \text{otherwise} \qquad\quad \text{(smooth stencil)}, \end{cases} \tag{21}$$

   where ϵ_{MR} is a user tunable parameter. (Typically $\epsilon_{MR} = 1 \times 10^{-3} \backsim 5 \times 10^{-2}$.)
3. A buffer zone is created around each grid point x_i that all the grid points inside the buffer zone are flagged as non-smooth stencils. This condition prevents the computation of the derivative of the fluxes by the FC method using non-smooth functional value.
   If, for example, a grid point x_i is flagged as a non-smooth stencil, then its neighboring grid points $\{x_{i-m}, \ldots, x_i, \ldots, x_{i+m}\}$ will also be designated as non-smooth stencils as well, that is, $\{\text{Flag}_j = 1, j = i-m, \ldots, i, \ldots, i+m\}$. (Typically, $m = r$.)
4. Use the FC method to compute the derivative of the fluxes in each segment of smooth stencils of data length N according to the procedure outlined in [27].
5. Use the WENO-Z scheme to compute the derivative of the fluxes for the remaining grid points.

The resulting system of ODEs resulted from the spatial discretization is advanced in time via the third order TVD Runge-Kutta scheme [2]. The CFL condition is set to be CFL = 0.4 in this study. The eighth order finite difference filtering is applied to the smooth stencils at the end of each Runge-Kutta step to stabilize the Hybrid scheme. We would like to note that the optimal order of the Hybrid scheme as designed is bounded by the optimal order of the WENO-Z scheme, which is fifth order in this case.

4. Numerical results and discussion

In this section, we evaluate the performance of the Hybrid scheme in simulating a *long time* evolution of the detonation front and its associated fine scale structures by several classical two- and three-dimensional examples.

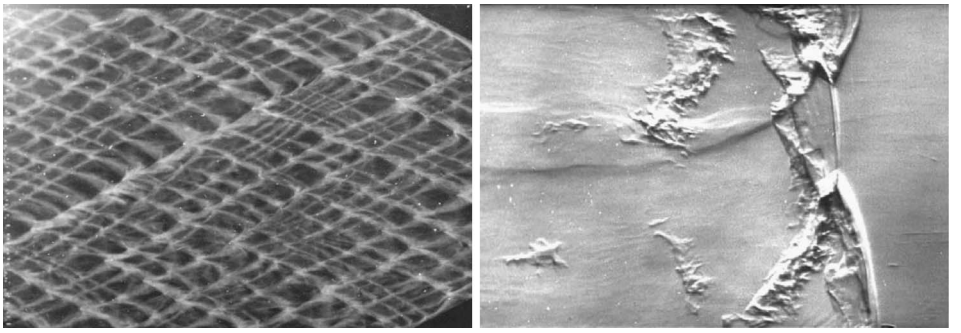

Figure 3: (Left): Open-shutter photograph and (Right): Schlieren photograph of the detonation in a thin channel [26] pp. 184–185.

4.1. 2D detonation wave simulations

It is well-known that all the realistic detonation phenomena are essentially three-dimensional, but many important essential detonation structures can be observed from the two-dimensional simulations, such as the regular or irregular cellular structures, triple-shock Mach intersection in the shock interface, unburned pockets behind the leading front. Furthermore, the results of two-dimensional simulations usually provide valuable reference for the three-dimensional simulations. For example, Fig. 3 shows an open-shutter photograph of the transverse wave trajectories for $C_2H_2 + 2.5O_2$ and a highly resolved schlieren photograph illustrating the detailed structures of the reaction zone for $CH_4 + 2O_2$ in a thin channel [26].

In this section, three classical detonations (Cases A, B and C in Table I.) are simulated. The computational domain is set to be $(x, y) = [0, 40] \times [-15, 15]$ with PML layer $(x, y) = [0, 6] \times [-15, 15]$ and the location of the initial detonation front at $x_d = 30$. The grid sizes are $N_x \times N_y = 800 \times 600$. $\epsilon_{MR} = 0.03, 0.03, 0.01$ are used in the Cases A, B and C respectively.

4.1.1. Case A: stable detonation The stiffness coefficient in this case is chosen as $K = 1134363.64$. The corresponding one-dimensional detonation wave is linearly stable. It allows the formation of the stable regular cellular structures.

To show the dissipation and dispersion properties, the contours of temperature computed by two schemes at time $t = 30$ are shown in Fig. 4 respectively. We observe more fine scale structures (for example, the small mushroom shaped vortical rollups along the slip line) in the flow field are

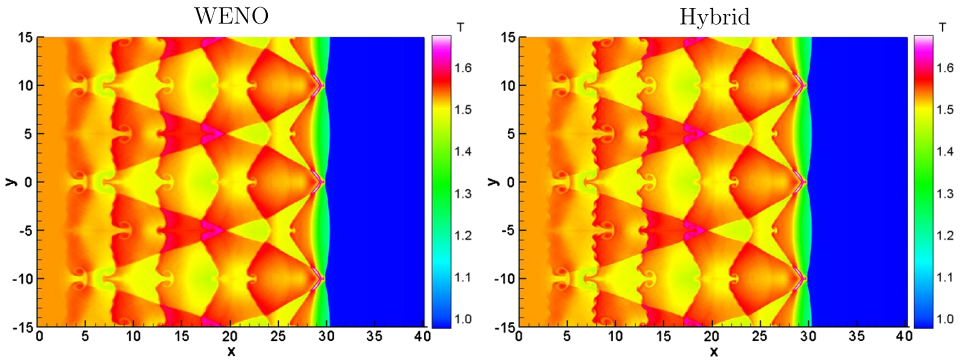

Figure 4: Case A: (Color online) The temperature T with the perturbed wave parameters ($k = 3,\ A = 0.1$) computed by (Left): the WENO-Z scheme and (Right): the Hybrid scheme.

more clearly resolved by the Hybrid scheme than those computed by the pure WENO-Z scheme.

The steady state contours of pressure and mass fraction at time $t = 260 \sim 268$ are shown in Fig. 5 in which the global structures near the detonation front agree well with those in the literature [3, 33]. From the pressure contours, the strength of the transverse wave is similar and interacts with shock front to form triple points (TPs). The TPs move perpendicular to the solid wall. The Mach stem and the incident wave alternatively appear on the shock front. The contours of mass fraction show that the combustion front evolves in a regular manner in time and space.

Fig. 6 shows the temporal evolution of the peak pressure. The initial transverse waves are weak and propagate along the leading shock front with the same number as that in the initial conditions [3, 19]. With the detonation decaying, the transverse waves coalesce, reducing the total number of the transverse waves until reaching a steady state. At that time, the transverse waves are weak and propagate more or less at the acoustic velocity. The width-to-length ratio of the regular cellular pattern is about 0.55.

In Fig. 7, we show the steady state results computed by the Hybrid scheme with the periodical boundary condition in the y-direction, which was used extensively in the detonation simulations in a vast channel such as [3, 17, 19, 33, 44]. The temporal evolution of the cellular structure is very similar to those with the reflective boundary condition. An interesting phenomenon is found that the number of cellular structures in the y-direction is always an integer, but the width-to-length ratio is also about 0.55, which is the same as that with the reflective boundary condition before.

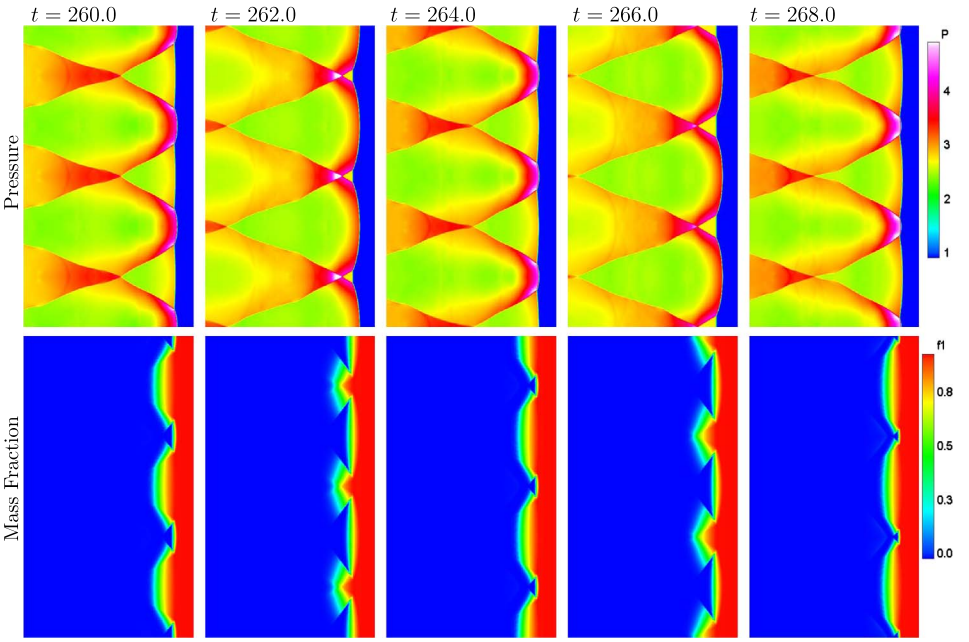

Figure 5: Case A: (Color online) The pressure P and mass fraction f_1 with the perturbed wave parameters ($k = 6,\ A = 0.1$) computed by the Hybrid scheme with $L_{1/2} = 20$.

Due to the unstable system, the external noises and any small perturbations might affect the evolution, formation and size of the cellular structures. Therefore, we investigate the effects of the initial conditions with different perturbed waves on the detonation structures. The temporal histories of the peak pressure with the initial perturbation wave parameters ($k = 15,\ A = 0.1$) and random initial perturbation waves computed by the Hybrid scheme are shown in Fig. 8 and Fig. 9 (only showing a representative one out of many realizations) respectively. Compared with Fig. 6, we observe that the initial conditions only play an important role in the initial transient phase of the formation of the cellular structures. The cellular structures at the final steady state does not depend on the randomness of the initial perturbation and are similar to those presented in Fig. 6. We also conduct many examples with random perturbations and obtain a similar observation. Moreover, the width-to-length ratio of the cellular structures is always $0.52 \sim 0.55$.

Hence, we conclude that an unstable cellular detonation structure after reaching the steady state solution is extremely robust and the external noise and boundary conditions do not influence the final steady state solu-

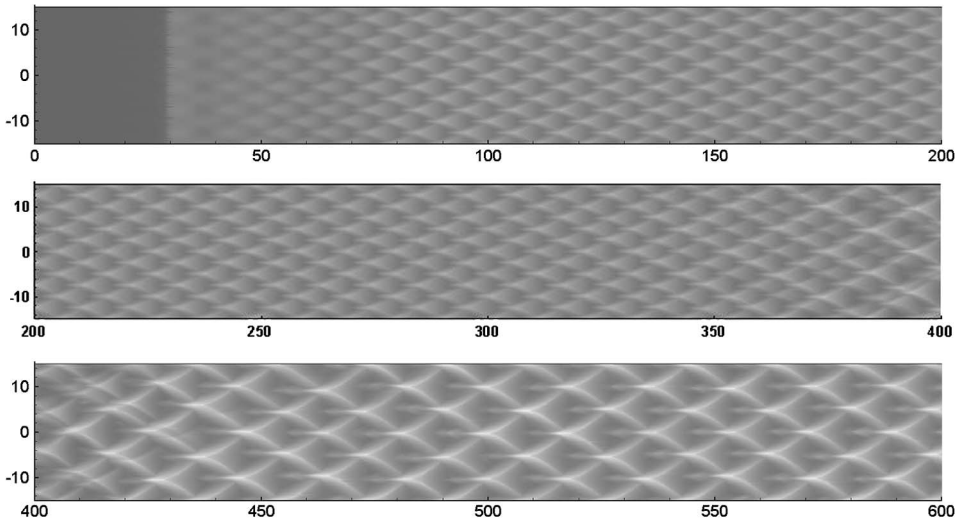

Figure 6: Case A: The history of the peak pressure with the perturbed wave parameters ($k = 6,\ A = 0.1$) with reflective boundary condition in the y-direction.

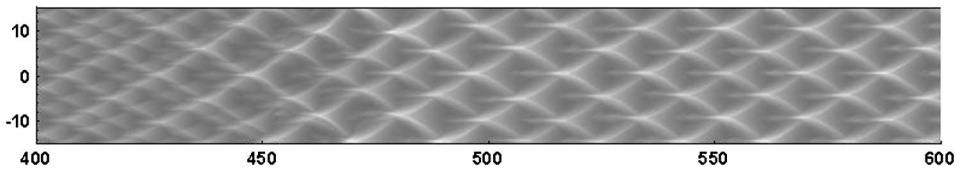

Figure 7: Case A: The history of the peak pressure with the perturbed wave parameters ($k = 6,\ A = 0.1$) (from $x = 400$ to $x = 600$) with the periodical boundary condition in the y-direction.

tion. Therefore, we use the parameters ($k = 6,\ A = 0.1$) and the reflective boundary condition in the y-direction in the following examples.

4.1.2. Case B: weakly unstable detonation We evaluate the performance of the Hybrid scheme by considering the weakly unstable case in this part. The pre-exponential parameter is set to be $K = 230.75$. The corresponding one-dimensional flow is linearly unstable with one unstable mode.

We first show the contours of pressure and mass fraction in Fig. 10 when the detonation wave reaches the steady state solution at time $t = 60 \sim 66$. From Fig. 10, we observe that the curvature of the leading front is larger and

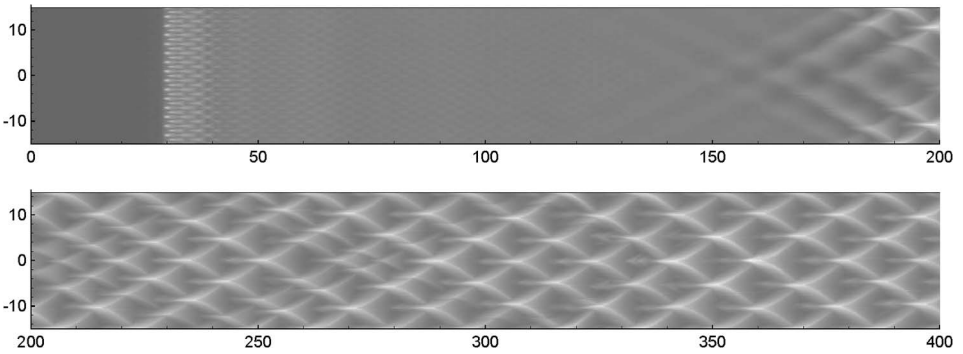

Figure 8: Case A: The temporal history of the peak pressure with the perturbed wave parameters ($k = 15,\ A = 0.1$).

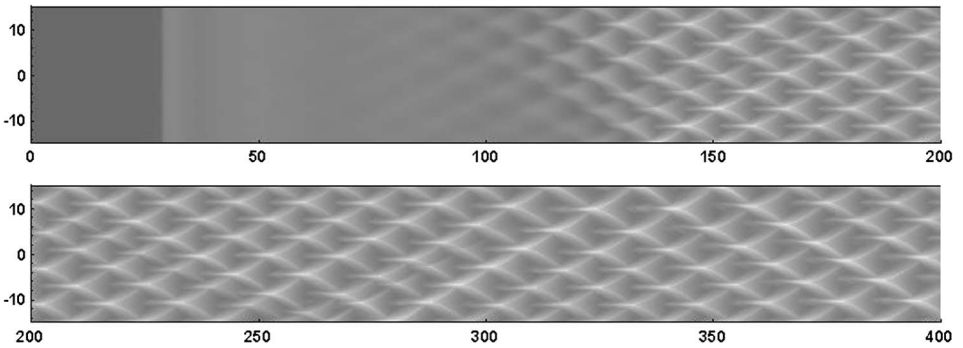

Figure 9: Case A: The temporal history of the peak pressure with a random perturbation.

the flow field in its wake has more complex structures than those in Case A. The transverse waves emanating from the TPs interact with each other as well as the burning gas inside the reaction zone. The interactions result in the formation of the un-reacted gas pockets, which burn at subsequent times and generate the compression waves, which further interact with the structures of front.

The cellular pattern shown in Fig. 11 is more irregular and complex than those in Case A. We can also observe that the transverse waves disappear when they coalesce and spontaneously appearing due to the rapid growth of small perturbations from instabilities around time $t = 180$. However, the averaged number of transverse waves in the y-direction remains the same as that in Case A.

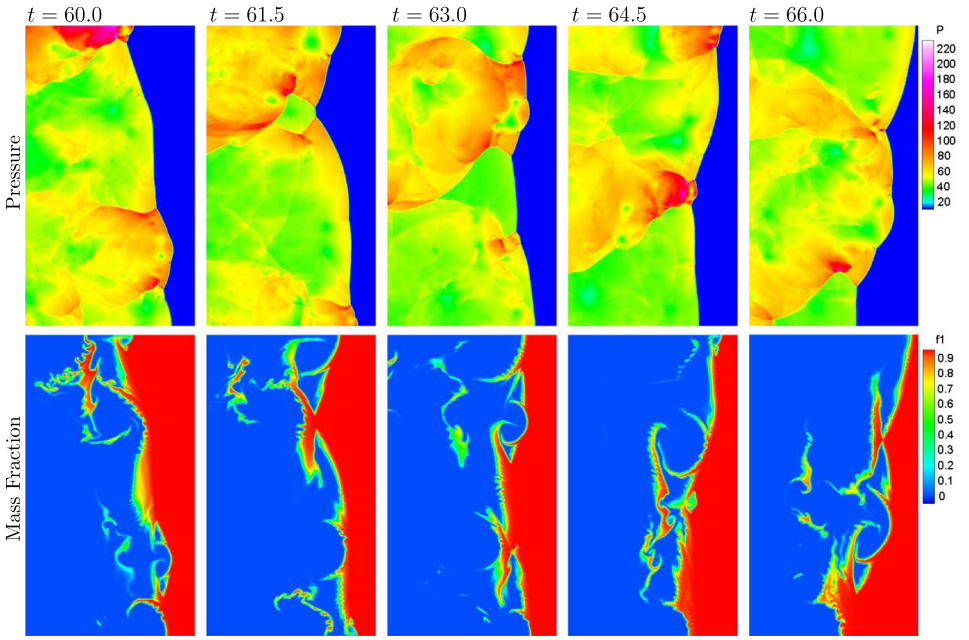

Figure 10: Case B: (Color online) The pressure P and mass fraction f_1 under the perturbation waves with parameters ($k = 6,\ A = 0.1$) computed by the Hybrid scheme with $L_{1/2} = 20$.

4.1.3. Case C: highly unstable detonation This case is an example of a highly unstable detonation with the pre-exponential parameter $K = 871.42$. According to the linear stability analysis, the corresponding one-dimensional case has five unstable modes. Two-dimensional linear stability studies reveal that the corresponding two-dimensional flow is unstable at arbitrarily short wavelengths.

In Fig. 12 and Fig. 13, we show the structures of pressure and mass fraction at time $t = 147 \sim 155$ near the detonation front and temporal history of the peak pressure respectively. In the early stages, the evolution of the flow-field resembles the equivalent one-dimensional process. More specifically, the shock pressure and temperature drop below the ZND values and, as a consequence, the reaction zone stays temporarily behind the hydrodynamic shock. Later on, material burns fast due to the thermal runaway, resulting in high over-pressure. It suggests that in the early times the evolution process is dominated by longitudinal instabilities. Once the transverse instabilities grow and start dominating the flow, the structures of flow field become increasingly chaotic. However, the transverse waves appear and disappear very quickly in

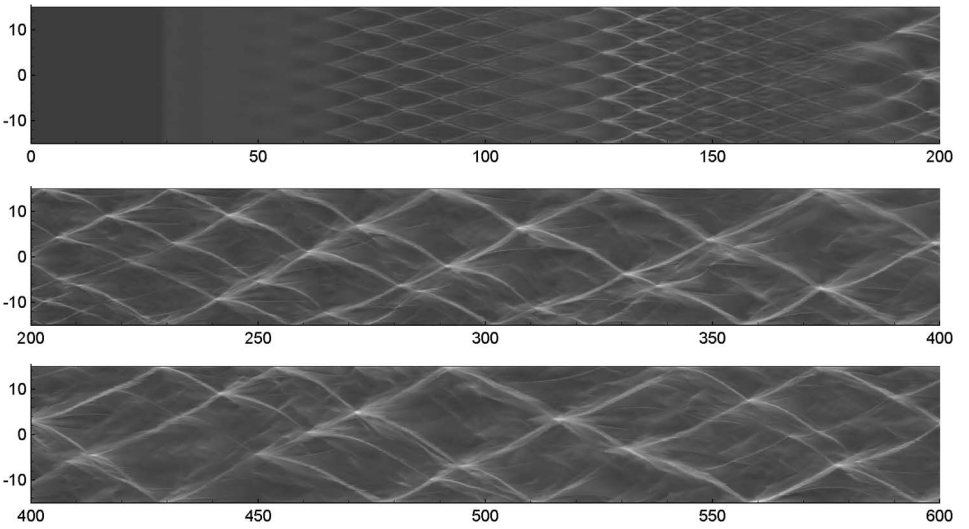

Figure 11: Case B: The history of the peak pressure with the perturbed wave parameters ($k = 6,\ A = 0.1$).

this case, the number of TPs on the shock front is no longer fixed and difficult to estimate. There are one or two very strong transverse waves, which mainly depend on the structures near the front. In the wake of front, there are many vortical structures. The pockets of unreacted material are constantly created and subsequently burn. Sometimes they can span the width of the channel. Furthermore, from the contours of mass fraction, we find that the combustion zone is narrower compared with case B. The transverse-wave collisions are happening more frequently. The shock wave systems resulting from those collisions interact with the vortical structures that have been convected downstream from the main front. Similar phenomena were observed and have been reported in [3, 33].

4.1.4. Efficiency of the Hybrid scheme Generally speaking, the Hybrid scheme should be faster than the pure WENO-Z scheme. However, as we know, the overall efficiency of the Hybrid scheme depends on the problems. In some particular problems containing complex flow structures, the Hybrid scheme might not achieve the computational efficiency due to the increase of the percentage of WENO region in the computational domain.

To gain a better understanding of the efficiency of the Hybrid scheme for the class of problems and setup in this study, we show the CPU time and the

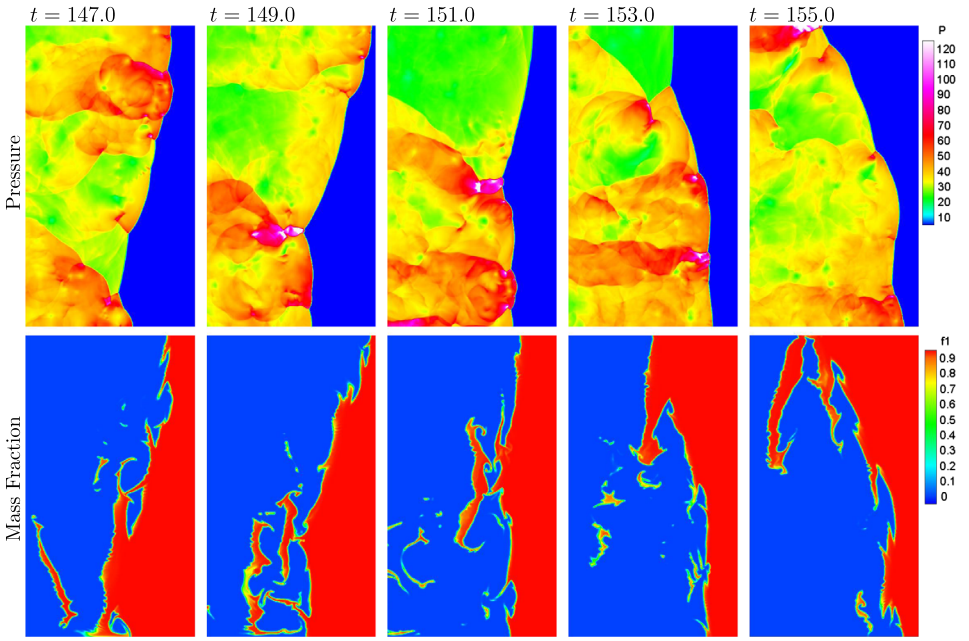

Figure 12: Case C: (Color online) The pressure P and mass fraction f_1 under the perturbation waves with parameters ($k = 6,\ A = 0.1$) computed by the Hybrid scheme with $L_{1/2} = 20$.

percentage of WENO region in the computational domain in Fig. 14 respectively. One can easily observe that the Hybrid scheme is more efficient than the pure WENO-Z scheme for Cases A and B. Moreover, the Hybrid scheme uses roughly the same amount of CPU time to that of the pure WENO-Z scheme in Case C. From Fig. 14, we conclude that when the percentage of WENO region increases, the efficiency of the Hybrid scheme decreases. The corresponding WENO Flags of three cases used in one Runge-Kutta stage also shown in Fig. 15.

4.2. 3D detonation wave simulations

In the 1960s, the experiments revealed that the gas-phase detonations were most often characterized by unsteady, three-dimensional structures. Therefore, in this part, we consider a stable three-dimensional detonation wave using the parameters of Case A, which can generate the in-phase rectangular, out-of-phase rectangular and in-phase diagonal detonations in the experiments, for investigating the performances of the Hybrid scheme.

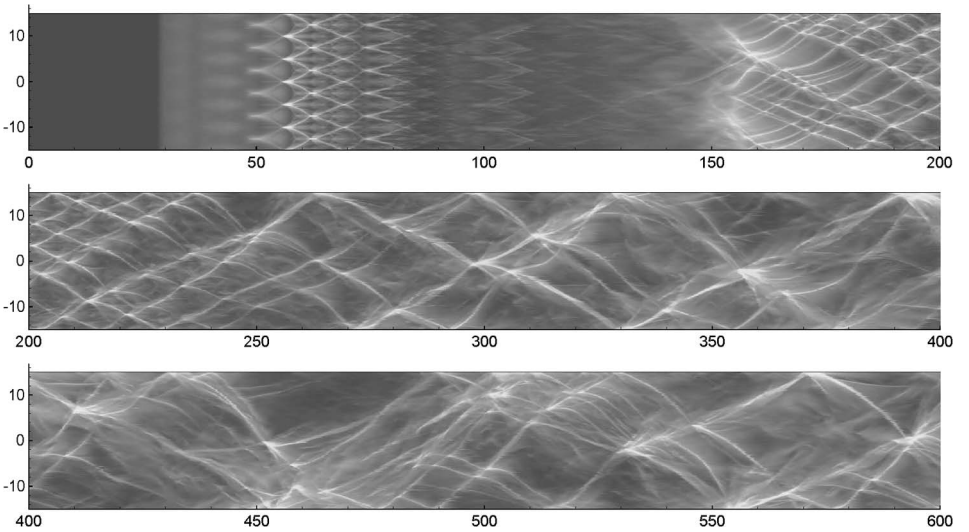

Figure 13: Case C: The history of the peak pressure with the perturbed wave parameters ($k = 6,\ A = 0.1$).

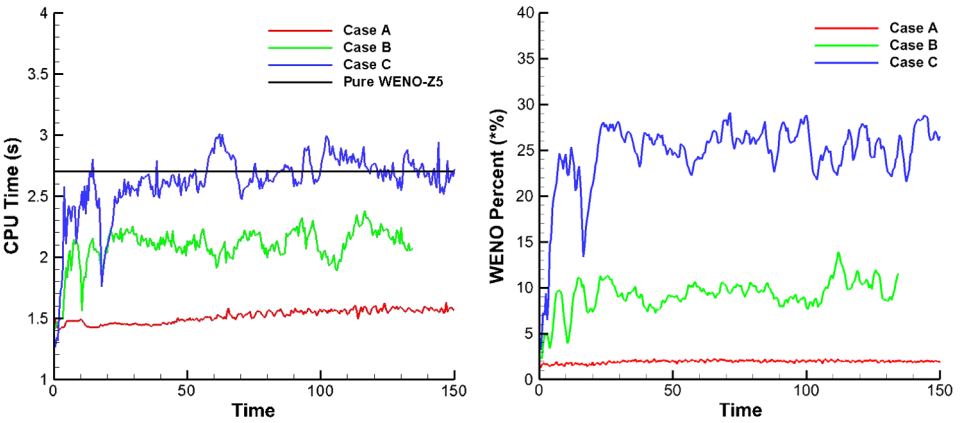

Figure 14: (Left) The CPU time used and (Right) percentage of WENO region in one Runge-Kutta stage of three cases.

The perturbation waves with parameters ($k = 2,\ A = 0.5$) and $\theta_1 = \theta_2 = 0$ are imposed on y- and z-directions respectively. The computational domain is set to be $(x, y, z) = [170, 200] \times [-10, 10] \times [-10, 10]$, and PML layer is $(x, y, z) = [170, 176] \times [-10, 10] \times [-10, 10]$. The number of grid points are $N_x \times N_y \times N_z = 300 \times 100 \times 100$. The detonation front is initially located

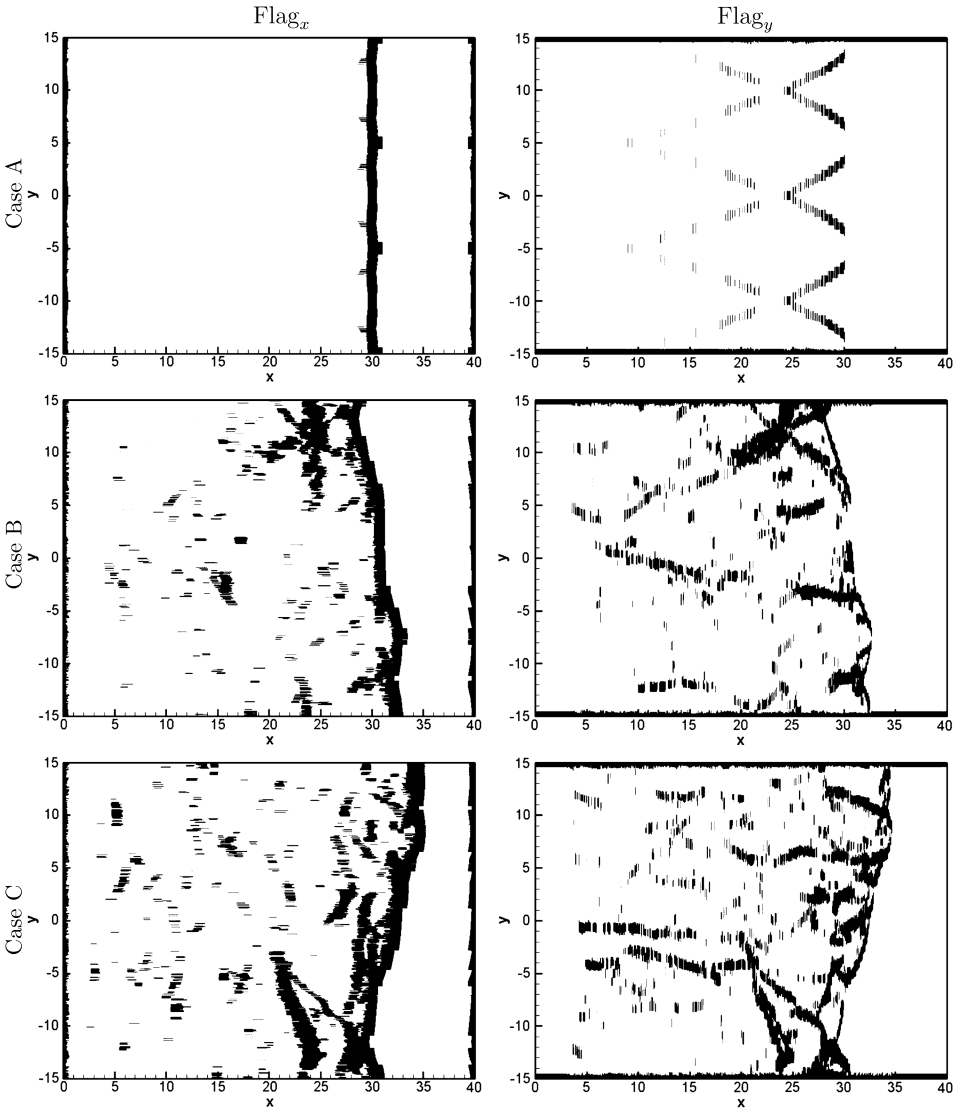

Figure 15: The WENO flags in x- and y-directions for cases A, B and C at the steady state.

at $x_d = 195$. We choose $\epsilon_{MR} = 0.03$ for this case. The history of the peak pressure on the walls of the in-phase rectangular, out-of-phase rectangular and in-phase diagonal detonations are shown in Fig. 16 which are in a good agreement with those in [9, 40, 43].

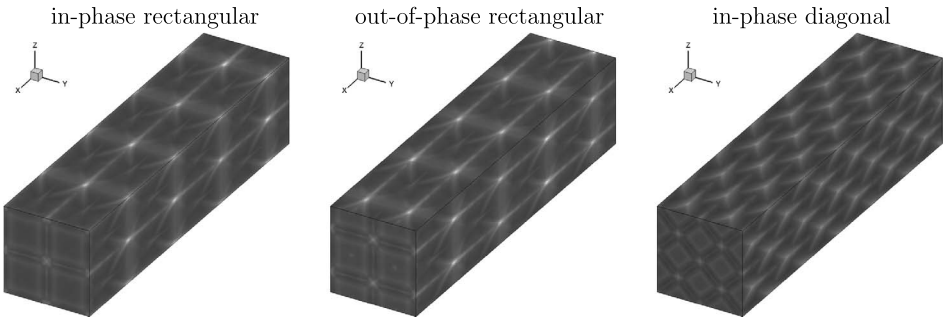

Figure 16: The history of the peak pressure on the walls: (Left) in-phase rectangular, (Middle) out-of-phase rectangular and (Right) in-phase diagonal detonations.

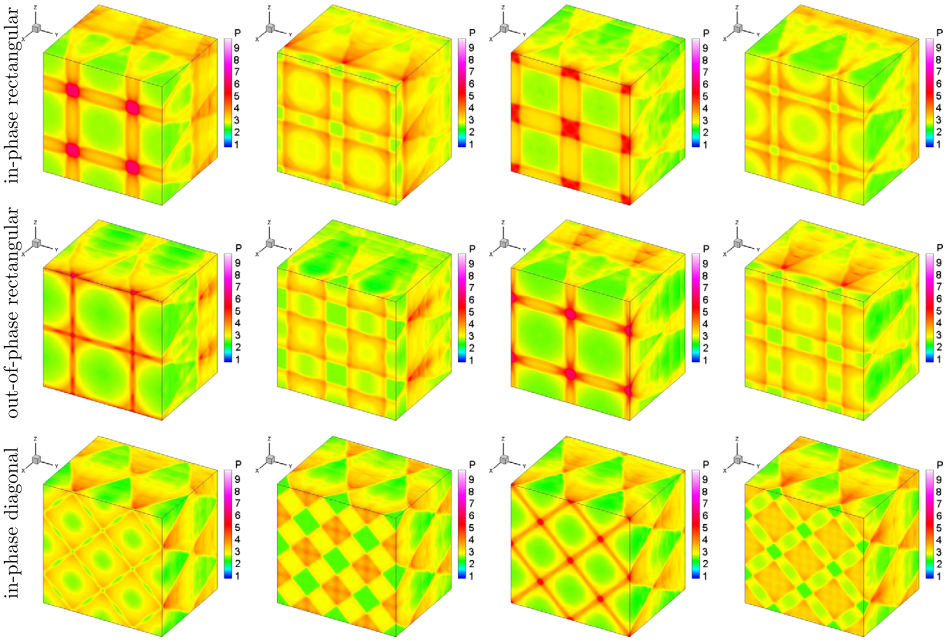

Figure 17: The front structure and pressure on the walls in one periodic: (Top) in-phase rectangular, (Middle) out-of-phase rectangular and (Bottom) in-phase diagonal detonation.

- In-phase rectangular
  We show the in-phase rectangular detonation in the top figure of Fig. 17. We observe that the detonation front contains four pairs of triple point

lines (TPLs), and each pair is parallel to the y- and z-directions respectively. When the TPLs collide with the walls, the slapping waves are formed on the walls (see the left figure of Fig. 16). Due to the same perturbation waves mode used in the y- and z-directions, the TPLs arrive at the walls simultaneously.

- Out-of-phase rectangular
  To generate the out-of-phase rectangular detonation, the transverse sine perturbation waves with different phases are imposed on the y- and z-directions (e.g. $\theta_1 = 0$ and $\theta_2 = \pi$ in this study) respectively. In the middle figure of Fig. 17 shows the pressure and the front structure on the walls for the out-of-phase rectangular detonation. We find that the cellular structures are similar to those generated in the in-phase case.
- In-phase diagonal
  We impose a symmetrical perturbation with period two along the diagonal direction where the pressure and density are increased by a factor of five. The bottom figure of Fig. 17 displays an evolution of a typical diagonal structure of the detonation front in one full period. The results show that the TPLs, moving along the diagonal direction, do not collide perpendicularly with the walls. Hence, the slapping waves on the walls disappear (see the right figure of Fig. 16). These results are in a very good agreement with those given in the literature [9, 40, 43]. Under this configuration, the detonation waves propagate in an in-phase diagonal mode, and the detonation front maintains a diagonal structure in a long time simulation.

5. Conclusion and future work

In this work, we study the performance of the hybrid FC-WENO-Z finite difference (Hybrid) scheme in the simulation of multi-dimensional detonation waves. The Hybrid scheme is used to keep the solutions parts displaying high gradients and discontinuities always captured by the WENO-Z scheme in an essentially non-oscillatory manner while the smooth parts are highly resolved by a linear, essentially non-dissipative and non-dispersive Fourier Continuation method. To detect the smoothness of the solutions, a high order multi-resolution algorithm by Harten is used.

For three classical two-dimensional cases, we show the cellular structures of detonations generated by imposing a transversely sinusoidal wave on a strong planar shock wave as a source of initial fluctuations. The structures behind the detonation front and cellular structures along the channel formed by the propagation of detonation waves are presented. The numerical results

show that the initial fluctuations affect the cell formation process, but play a minor role in the cell size and regularity of the structures of the quasi-steady state solutions. The reflective and periodic boundary conditions behave similarly in the evolution of cellular structures. A stable two-dimensional detonation waves show that more fine scale structures of detonation waves are well resolved by the Hybrid scheme with less CPU times than the pure WENO-Z scheme. We observe that the transverse waves emanate from the triple points interact with each other as well as the burning gas inside the reaction zone. These interactions result in the formation of the unburned gas pockets for the unstable detonations. The in-phase rectangular, out-of-phase rectangular and in-phase diagonal cellular structures are observed in the three-dimensional examples. The in-phase and out-of-phase slapping waves are also found in the rectangular detonations.

Our future work in this research area, we will perform more three-dimensional high resolution detonation wave simulations with multi-species undergoing a chain of chemical reactions using the Hybrid scheme in a parallel computer. We will also simulate the process of detonation under the multi-domain framework of reactive Navier-Stokes system in a complex geometry.

Acknowledgments

The authors would like to acknowledge the funding support of this research by National Natural Science Foundation of China (11801383, 11871443), National Science and Technology Major Project (20101010), Shandong Provincial Natural Science Foundation (ZR2017MA016) and Fundamental Research Funds for the Central Universities (201562012). The author (Don) also likes to thank the Ocean University of China for providing the startup fund (201712011) that is used in supporting this work.

References

[1] B. N. Azarenok and T. Tang, *Second-order Godunov-type scheme for reactive flow calculations on moving meshes*, J. Comput. Phys. **206** (2005), pp. 48–80. MR2135835

[2] R. Borges, M. Carmona, B. Costa, and W. S. Don, *An improved weighted essentially non-oscillatory scheme for hyperbolic conservation laws*, J. Comput. Phys. **227** (2008), pp. 3101–3211. MR2392730

[3] A. Bourlioux and A. J. Majda, *Theoretical and Numerical Structure for Unstable Two-Dimensional Detonations*, Combust. Flame **90** (1992), pp. 211–229.

[4] A. Bourlioux, A. J. Majda, and V. Roytburd, *Theoretical and Numerical Structure for Unstable One-Dimensional Detonations*, SIAM J. Appl. Math. **51** (1991), pp. 303–343. MR1095022

[5] O. P. Bruno and M. Lyon, *High-order unconditionally stable FC-AD solvers for general smooth domains I. Basic elements*, J. Comput. Phys. **229** (2010), pp. 2009–2033. MR2586234

[6] M. Castro, B. Costa, and W. S. Don, *High order weighted essentially non-oscillatory WENO-Z schemes for hyperbolic conservation laws*, J. Comput. Phys. **230** (2011), pp. 1766–1792. MR2764010

[7] B. Costa and W. S. Don, *High order Hybrid Central-WENO finite difference scheme for conservation laws*, J. Comput. Appl. Math. **204** (2) (2007), pp. 209–218. MR2324451

[8] G. Dahlquist and A. Björk, *Numerical Methods*, Prentice Hall, Englewood Clis, 1974. MR0368379

[9] V. Deledicque and M. V. Papalexandris, *Computational study of three-dimensional gaseous detonation structures*, Combust. Flame **144** (2006), pp. 821–837.

[10] W. S. Don, *Numerical Study of Pseudospectral Methods in Shock Wave Applications*, J. Comput. Phys. **110** (1994), pp. 103–111.

[11] W. S. Don and R. Borges, *Accuracy of the Weighted Essentially Non-Oscillatory Conservative Finite Difference Schemes*, J. Comput. Phys. **250** (2013), pp. 347–372. MR3079539

[12] H. S. Dou, H. M. Tsai, B. C. Khoo, and J. X. Qiu, *Simulations of detonation wave propagation in rectangular ducts using a three-dimensional WENO scheme*, Combust. Flame **154** (2008), pp. 644–659.

[13] W. Fickett and W. C. Davis, *Detonation*, Univ. California Press, 1979.

[14] V. N. Gamezo, A. A. Vasilév, A. M. Khokhlov, and E. S. Oran, *Fine Cellular Structures Produced by Marginal Detonations*, Proc. Combust. Inst. **28** (2000), pp. 611–617.

[15] V. N. Gamezo, D. Desbordes, and E. S. Oran, *Two-Dimensional Reactive Flow Dynamics in Cellular Detonation Waves*, Shock Waves **9** (1999), pp. 11–17.

[16] V. N. Gamezo, D. Desbordes, and E. S. Oran, *Formation and Evolution of Two-dimensional Cellular Detonations*, Combust. Flame **116** (1999), pp. 154–165.

[17] Z. Gao and W. S. Don, *Mapped Hybrid Central-WENO Finite Difference Scheme for Detonation Waves Simulations*, J. Sci. Comput. **55** (2013) 351–371. MR3044178

[18] Z. Gao, W. S. Don, and Z. Q. Li, *High Order Weighted Essentially Non-Oscillation Schemes for One-Dimensional Detonation Wave Simulations*, J. Comput. Math. **29** (2011), pp. 623–638. MR2869424

[19] Z. Gao, W. S. Don, and Z. Q. Li, *High Order Weighted Essentially Non-Oscillation Schemes for Two-Dimensional Detonation Wave Simulations*, J. Sci. Comput. **53** (2012), pp. 80–101. MR2965306

[20] D. Gottlieb and S. Orzag, *Numerical analysis of spectral methods: Theory and applications*, SIAM (1977). MR0520152

[21] A. Harten, *High resolution schemes for hyperbolic conservation laws*, J. Comput. Phys. **49** (1983), pp. 357–393. MR0701178

[22] X. Y. Hu, B. C. Khoo, D. L. Zhang, and Z. L. Jiang, *The cellular structure of a two-dimensional H2/O2/Ar detonation wave*, Combust. Theory Modelling **8** (2004), pp. 339–359.

[23] F. Jia, Z. Gao, and W. S. Don, *A Spectral Study on the Dissipation and Dispersion of the WENO schemes*, J. Sci. Comput. **63** (2015), pp. 49–77. MR3315268

[24] G. S. Jiang and C. W. Shu, *Efficient Implementation of Weighted ENO Schemes*, J. Comput. Phys. **126** (1996), pp. 202–228. MR1391627

[25] D. A. Kessler, V. N. Gamezo, and E. S. Oran, *Multilevel Detonation Cell Structures in Methane-Air Mixtures*, Proc. Combust. Inst. **33** (2011), pp. 2211–2218.

[26] John H. S. Lee, *The Detonation Phenomenon*, Cambridge University Press, (2008), pp. 98–139.

[27] P. Li, Z. Gao, W. S. Don, and S. S. Xie, *Hybrid Fourier-Continuation Method and Weighted Essentially Non-oscillatory Finite Difference Scheme for Hyperbolic Conservation Laws in a Single-Domain Framework*, J. Sci. Comput. **64** (2015), pp. 670–695. MR3377834

[28] Z. Liang and L. Bauwens, *Cell structure and stability of detonations with a pressure-dependent chain-branching reaction rate model*, Combust. Theory Modelling **9** (2005), pp. 93–112. MR2175165

[29] Z. Liang and L. Bauwens, *Detonation structure with pressure-dependent chain-branching kinetics*, Proc. Combust. Inst. **30** (2005), pp. 1879–1887.

[30] C. V. Loan, *Computational Frameworks for the Fast Fourier Transform*, SIAM (1992). MR1153025

[31] M. Lyon and O. P. Bruno, *High-order unconditionally stable FC-AD solvers for general smooth domains II. Elliptic, parabolic and hyperbolic PDEs; theoretical considerations*, J. Comput. Phys. **229** (2010), pp. 3358–3381. MR2601104

[32] M. V. Papalexandris, A. Leonard, and P. E. Dimotakis, *Unsplit schemes for hyperbolic conservation laws with source terms in one space detonation*, J. Comput. Phys. **134** (1997), pp. 31–61. MR1455254

[33] M. V. Papalexandris, A. Leonard, and P. E. Dimotakis, *Unsplit Algorithms for Multidimensional System of Hyperbolic Conservation Laws with Source Terms*, Comput. Math. Appl. **44** (2002), pp. 25–49. MR1908268

[34] J. J. Quirk, *Godunov-type schemes applied to detonation flows*, ICASE Report **93** (1993), 15.

[35] K. Shahbazi, N. Albin, O. Bruno, and J. S. Hesthaven, *Multi-domain Fourier-continuation/WENO hybrid solver for conservation laws*, J. Comput. Phys. **230** (2011), pp. 8779–8796. MR2845019

[36] K. Shahbazi, J. S. Hesthaven, and X. Y. Zhu, *Multi-dimensional hybrid Fourier continuation-CWENO solvers for conservation laws*, J. Comput. Phys. **253** (2013), pp. 209–225. MR3193395

[37] F. Sharpe and S. A. E. G. Sharpe, *Two-dimensional numerical simulations of idealized detonations*, Proc. R. Soc. Lond. A **456** (2000), pp. 2081–2100. MR1794717

[38] M. Short and G. J. Sharpe, *Pulsating instability of detonations with a two-step chain-branching reaction model: theory and numerics*, Combust. Theory Modelling **7** (2003), pp. 401–416. MR1988455

[39] N. Tsuboi, Y. Daimon, and A. K. Hayashi, *Three-dimensional numerical simulation of detonations in coaxial tubes*, Shock Waves **18** (2008), pp. 379–392.

[40] C. Wang, P. Li, Z. Gao, and W. S. Don, *Three-Dimensional Detonation Simulations with the Mapped WENO-Z Finite Difference Scheme*, Comput. Fluids, doi:10.1016/j.compfluid.2016.04.016, in press. MR3556307

[41] C. Wang, J. G. Ning, and J. Lei, *Numerical Study on Propagation of Explosion Wave in H2-O2 Mixtures*, Adv. Nat. Comput. **4222** (2006), pp. 816–819.

[42] C. Wang, J. G. Ning, and T. B. Ma, *Numerical simulation of Detonation and Multi-Material Interface Tracking*, Comput. Mater. Con. **22** (2011), pp. 73–96.

[43] C. Wang, C.-W. Shu, W. H. Han, and J. G. Ning, *High resolution WENO simulation of 3D detonation waves*, Combust. Flame **160**(2) (2013), pp. 447–462.

[44] Z. C. Zhang, S. T. Yu, H. He, and S. C. Chang, *Direct calculation of two- and three- dimensional detonations by an extended CE/SE method*, AIAA Paper (2001), pp. 2001–0476.

Peng Li
Department of Mathematics and Physics
Shijiazhuang Tiedao University
Shijiazhuang
China
E-mail: weilailp@163.com

Zhen Gao
School of Mathematical Sciences
Ocean University of China
Qingdao
China
E-mail: zhengao@ouc.edu.cn

Wai Sun Don
School of Mathematical Sciences
Ocean University of China
Qingdao
China
E-mail: waisundon@gmail.com